Materials Advances

ROYAL SOCIETY OF CHEMISTRY

PAPER

View Article Online
View Journal | View Issue

Cite this: *Mater. Adv.*, 2025, **6**, 7443

Formation of the (Ti,V)(C,N) solid solutions by HPHT sintering of mechanically alloyed TiC–VN powder mixtures

N. M. Belyavina, [a] V. V. Kuryliuk, *[a] A. M. Kuryliuk, [a] D. A. Stratiichuk, [b] S. P. Starik [bc] and O. I. Nakonechna [d]

Received 24th July 2025,
Accepted 12th September 2025

DOI: 10.1039/d5ma00805k

rsc.li/materials-advances

Nanocrystalline solid solutions of $Ti_{1-x}V_xC_{0.5}N_{0.5}$ (x = 0.4–0.6) were synthesized by HPHT sintering (7.7 GPa, 2150 °C) of TiC–VN powder mixtures (molar ratios 2 : 1, 1 : 1, and 1 : 2), which had undergone preliminary 9-hour mechanochemical processing in a high-energy planetary ball mill until the formation of (Ti,V)C and (V,Ti)N solid solutions. The resulting compacts possess homogeneous microstructure, which was confirmed by XRD, SEM and EDS studies. Composition of the sintered solid solutions corresponds to the original TiC–VN blends, while their lattice parameters fit well into the linear dependence of Vegard's law. The $Ti_{1-x}V_xC_{0.5}N_{0.5}$ solid solutions remain stable after annealing for 2 hours at 800 °C. The Vickers microhardness measurements were carried out, with the hardness values monotonically varying between those typical for TiC and VN phases. The proposed two-step method (mechanochemical activation followed by high-pressure sintering) enables the synthesis of composites containing nanocrystalline solid solutions of a predetermined composition.

Introduction

TiC and VN refractory compounds are characterized by unique physical and chemical properties such as high melting point, chemical stability, hardness, and good thermal, electrical, and optical characteristics, making them widely used in many industrial fields.[1–3] In particular, TiC and VN have found successful application as individual dopants to improve the functional properties of PcBN ceramics based on cubic boron nitride (cBN),[4–6] and also to enhance the performance of medical titanium alloys.[7,8] It has also been shown that the use of PcBN material with a two-phase filler, in which TiC is combined with VN, leads to a significant increase in wear resistance of cutting tools during high-speed machining of nickel-based superalloys such as Inconel 718 and stainless steel AISI 316L.[9] It is assumed that the formation of multicomponent solid solutions (Ti,V)(C,N) and (V,Ti)N in the sintered products may lead to the improved performance of this material.[10]

It should be noted that many binary carbides and nitrides with NaCl-type structures are prone to forming mutual solid solutions.[11] In some cases, the properties of such multicomponent phases exceed those of the binary compounds that create them. For example, $Ti_{0.6}Hf_{0.4}C$ carbide is one of the hardest materials known (43.1 GPa),[12] while Ti(C,N) compound significantly improves the strength and wear resistance of a broad class of ceramic materials.[13]

However, many multicomponent carbides, nitrides, or carbonitrides still require developing synthesis conditions and studying the characteristics of materials obtained. For instance, a high-entropy (Ta,Zr,Nb)C carbide with a hardness of approximately 34 GPa was obtained using spark plasma sintering,[14] while (Hf,Zr,Ti,Ta,Nb)C carbide was synthesized using hot pressing at 1900 °C.[15] Quaternary carbonitrides $V_{1-x}Ti_x(C,N)$ ($0 \leq x \leq 0.4$) with NaCl-type structure have been synthesized *via* a carbothermal reduction–ammonolysis/carburization (MWCRAC) method under direct microwave heating and controlled atmospheres using a modified DMOreactor.[16] The reaction starting materials were vanadium and titanium oxides (V_2O_5, VO_2, TiO_2, and Ti_4O_7), with reduction, nitriding, and carburizing processes carried out in an NH3 atmosphere in the presence of amorphous carbon.

One effective method for synthesizing the multicomponent solid solutions is mechanical alloying (MA) of the initial powder mixtures in a planetary ball mill. Applying this method, Ti(C,N) compounds have been synthesized from metallic titanium, graphite, and TiN.[17] In our previous studies,[18–21] we mechanically alloyed the limited solid solutions (Zr,Ti)C, (Ti,V)N, (Ti,V)C, and (V,Ti)N from binary carbides and nitrides.

[a] *Taras Shevchenko National University of Kyiv, Kyiv, Ukraine. E-mail: kuryliuk@knu.ua*
[b] *V.N. Bakul Institute for Superhard Materials of NAS of Ukraine, Kyiv, Ukraine*
[c] *Frantsevich Institute for Problems of Materials Science of NAS of Ukraine, Kyiv, Ukraine*
[d] *Kairos Medical AG, Föhrenweg 9, 2544 Bettlach, Switzerland*

Given the positive effect of the TiC–VN two-phase binder on the performance characteristics of PcBN ceramic of cBN–TiC–VN–(Al) system,[9] this work aims to establish the effect of preliminary mechanochemical processing on the structure and performance characteristics of the HPHT-sintered TiC–VN mixtures.

Experimental details

The subjects of this study were compact samples obtained by HPHT sintering in a toroid-type high-pressure apparatus (V. Bakul Institute for Superhard Materials, Ukraine) equipped with a WC-Co anvil (DURIT Hartmetall GMBH, Germany) (pressure of 7.7 GPa, temperature of 2150 °C). Three TiC–VN treated powder mixtures with molar ratios of 2 : 1, 1 : 1, and 1 : 2 were used as charge, namely, TiC : VN 2 : 1, TiC : VN 1 : 1, and TiC : VN 1 : 2, respectively. Dispersed powders of TiC (99.9 wt% of purity) and VN (99.9 wt% of purity) with particle size about 50 μm served as initial components of the charge. Powder charge was processed for 9 hours in a high-energy planetary ball mill (Taras Shevchenko University, Ukraine) using 20 steel balls (10 mm of diameter, the mass ratio of the balls to powder was 20 : 1) at a rotation speed of 1400 rpm in a cyclic mode (20 min) of treatment and 10 min of cooling, kinetic of this synthesis is described in more details in ref. 20 and 21. Mechanically alloyed charge was HPHT sintered. Control samples were compacts obtained by HPHT sintering (7.7 GPa, temperatures of 1800 °C and 2150 °C) of an unprocessed TiC–VN (1 : 1) mixture.

X-ray diffraction (XRD) analysis of the powder mixtures prepared for sintering and the resulting compacts was performed using Shimadzu XRD-6000 (SHIMADZU, Japan) and DRON-3 M (Burevestnik factory, USSR) diffractometers (CuKα radiation) in a discrete mode under the following scanning parameters: observation range $2\theta = 20^\circ$–100°, step scan of 0.05° and counting time per step at 3 s. The original software package, including complete complex of standard Rietveld procedures, has been used for analysis and interpretation of the X-ray diffraction patterns obtained, namely, determination of both peak positions and integral intensities of the Bragg reflections by means of complete profile analysis; qualitative phase analysis using the least square method for lattice parameters refinement; refining crystal structures of phases (including atomic position filling) and calculation of the parameters of their real structure (coherent block sizes and microdeformation values). The full methodology is described in ref. 22 and available at X-ray.univ.kiev.ua.

The microstructure of the compacts was studied using a ZEISS EVO 50 XVP scanning electron microscope (Carl Zeiss Microscopy GmbH, Germany) in a material contrast mode using a phase-sensitive Compact Zeiss Backscattered Detector (CZ BSD) to collect backscattered electrons. Phase composition was determined *via* energy-dispersive X-ray spectroscopy (EDS) using an Ultim Max 100 analyzer (Oxford Instruments, UK) integrated into the SEM.

The Vickers microhardness of the samples was determined using an LHVS-1000Z (Chongqing Leeb Instrument Co Ltd, China) digital microhardness tester with a standard diamond pyramid indenter. Each sample was indented 50 times under a load of 0.3 kg for 10 seconds. After unloading, the diagonal of the resulting indentation was measured, and the hardness was calculated using the software provided with the tester. The Vickers hardness number (HV) was calculated as:

$$\mathrm{HV} = \frac{1854P}{d^2},$$

where P is the applied load in kilograms-force, d is the average length of the diagonals of the indentation in micrometers.

Results and discussion

X-ray diffraction

According to the results of X-ray diffraction phase analysis, the mechanically alloyed TiC–VN powder mixtures prepared for HPHT sintering are two-phase and contain mutual solid solutions of (Ti,V)C and (V,Ti)N (Fig. 1). According to XRD and EDS analyses, (Ti,V)C and (V,Ti)N contain approximately 16 at% V and Ti, respectively (see Table S1, SI for more details). A similar phase composition is observed in the HPHT-sintered products prepared from a TiC : VN 1 : 1 mixture not subjected to prior mechanical alloying (see Fig. S1 and Table S2, SI).

Analyzing the kinetics of phase transformations[21] showed that TiC and VN crystal structures undergo specific changes under impact loading at the MA of TiC–VN mixtures. In this case, at the initial stage of MA, the point defects – such as structural vacancies (in VN and TiC) and interstitial atoms (in TiC) – accumulate due to metal atoms being displaced from their sublattices. At the same time, the formation of vanadium and titanium clusters occur in the milling zone. Electronic structure studies[23] show that the density of states (DOS) profiles (for both the valence and conduction bands) of TiC and VN phases containing numerous vacancies are significantly broadened and exhibit additional peaks near the Fermi level. Altogether, these transformations indicate a high degree of structural instability, creating favorable conditions for forming solid solutions.

Such solid solutions of (Ti,V)C and (V,Ti)N form after 8–9 hours of mechanical alloying of TiC–VN powder mixtures in the high-energy planetary ball mill[21] (see Table S1, SI). DOS profiles of these solid solutions resemble those of the initial compounds but with more smoothed transitions between bands, indicating the possibility of further structural changes.[22]

The transformations occur after HPHT sintering (7.7 GPa and 2150 °C) of the mechanically alloyed TiC–VN mixtures. So, X-ray diffraction analysis of the HPHT sintered samples has revealed almost single-phase composition of materials studied (Fig. 1). The details of quaternary solid solutions with varying compositions formed at synthesis are listed in Table S2, SI.

Data on the lattice parameters of the original phases (TiC and VN) as well as (Ti,V)C, (V,Ti)N and (Ti,V)(C,N) solid

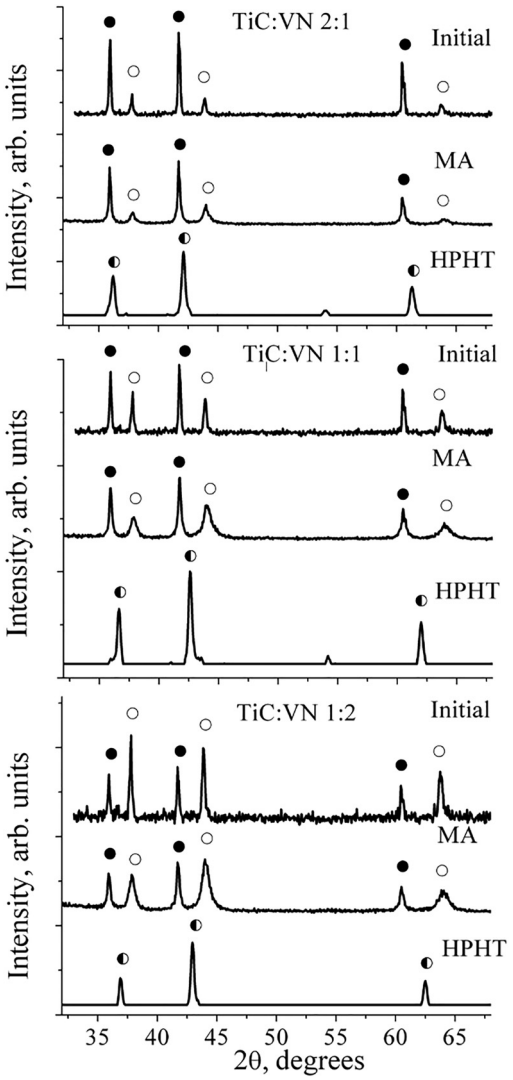

Fig. 1 Fragments of X-rays diffraction patterns of initial mixture, mechanically alloyed TiC–VN mixtures (MA) and HPHT sintered samples made of those MA powders. TiC phase is marked with ●, VN phase is marked with ○ and solid solution is marked with ◐.

solutions synthesized are shown in Fig. 2. It is evident (Fig. 2) that the lattice parameters of (Ti,V)C and (V,Ti)N ternary solid solutions are independent of the initial mixture composition, being determined instead by the duration of mechanical alloying treatment. The composition of these phases also does not depend on the mixture type (see Table S1, SI). However, the lattice parameters of the quaternary (Ti,V)(C,N) solid solutions follow a linear trend in accordance with Vegard's law (Fig. 2), indicating that the composition of these solid solutions corresponds to the initial mixture (at least in terms of the Ti to V ratio).

Scanning electron microscopy (SEM/EDS)

The mechanochemically treated TiC–VN mixtures prepared for sintering, as well as the HPHT-sintered samples subsequently annealed for 2 h at 800 °C, were examined by SEM. As can be

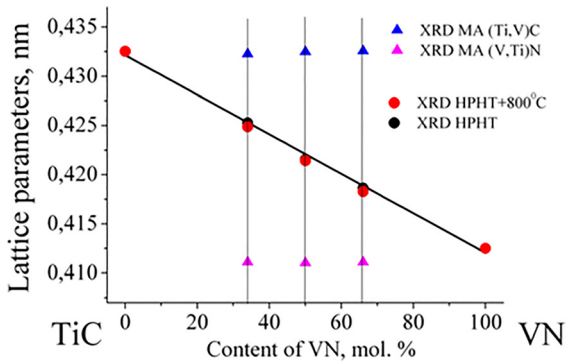

Fig. 2 Lattice parameters (circles) of HPHT sintered quaternary (Ti,V)(C,N) solid solutions and lattice parameters of ternary (Ti,V)C and (V,Ti)N solid solutions, existing in mechanically alloyed charge (triangles) in dependence on VN content.

seen from the SEM images (Fig. 3), the TiC–VN powder mixtures are predominantly fine-grained and, according to EDS analysis, consist of (V,Ti)N and (Ti,V)C phases (see Table S1, SI for details). The coarse grains observed in the TiC : VN 2 : 1 and TiC : VN 1 : 2 mixtures (Fig. 3a and c) correspond to unreacted V and Ti clusters, respectively. In addition, the TiC : VN 1 : 1 mixture contains a fraction of equiatomic (Ti,V)(C,N) grains.

The microstructure of the TiC : VN 1 : 1 sample is entirely homogeneous (Fig. 3a). However, the other two samples contain bright inclusions and islands of fine-grained phases (Fig. 3b and c). The main phase (gray field in Fig. 3) in the studied compacts is a quaternary (Ti,V)(C,N) solid solution of varying composition. The main elements – Ti, V, C, and N – are uniformly distributed (Fig. 4) in a sample. EDS data (Fig. 3) shows that the titanium and vanadium content align well with the initial mixture composition (see Table S2, SI).

Bright phase observed in the TiC : VN 1 : 1 and TiC : VN 1 : 2 samples (Fig. 3b and c) is identified as α-Fe, resulting from contamination the ball mill (steel balls and vials), which is also confirmed by XRD data. EDS maps (Fig. 4) show distinct iron distributions. Dark inclusions on the surface of the 1 : 1 and 1 : 2 samples (Fig. 3b and c) are interpreted as a mixture of carbon and VN with a lattice parameter $a \approx 0.4125$ nm. Annealing also results in the formation of TiO_2 oxide on the surface of the samples.

Microhardness measurements

Results of Vickers microhardness tests for HPHT sintered (7.7 GPa, 2150 °C) and annealed (800 °C, 2 hours) samples are shown in Fig. 5 as histograms of experimental data, processed using Gaussian statistical fitting. The resulting normal distribution curves are also presented (Fig. 5a), with key characteristics (mean and standard deviation) summarized in Table S3, SI.

The analysis shows that both HPHT sintered and annealed samples exhibit a symmetric normal distribution of microhardness values ($A = 0$). Annealing at 800 °C causes some curves (distributions) to shift toward lower hardness values and broaden, particularly for vanadium-rich compositions.

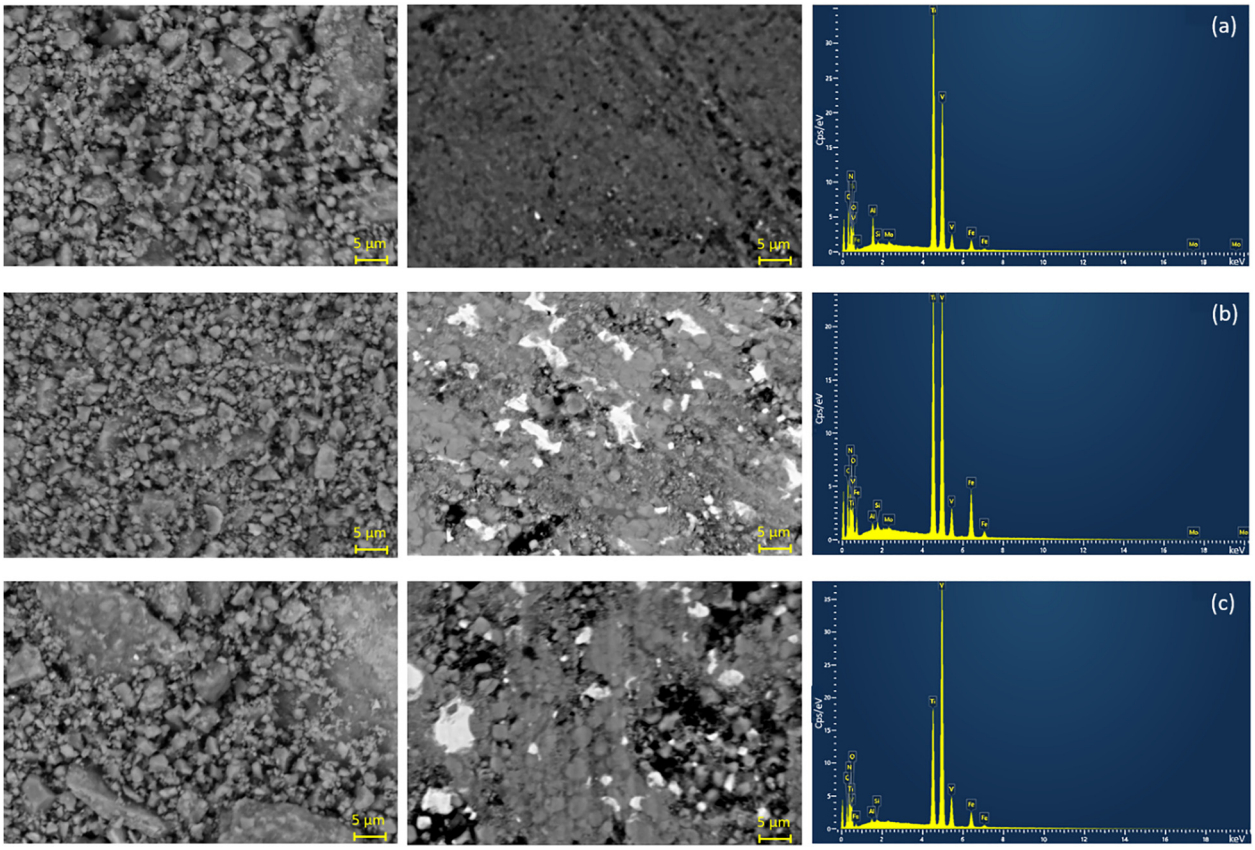

Fig. 3 SEM image (×5000) for the MA-treated TiC–VN powders and HPHT sintering samples after annealing at 800 °C as well as EDS spectra for compacts: TiC : VN 2 : 1 (a); TiC : VN 1 : 1 (b); TiC : VN 1 : 2 (c). Corresponding full-scale EDS spectra are available in the SI (Fig. S2–S4).

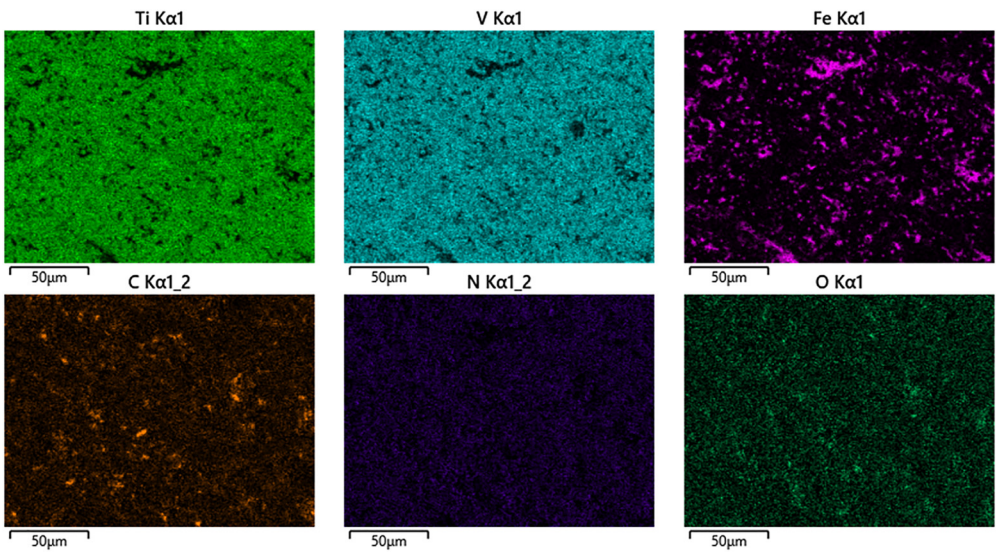

Fig. 4 Elemental maps for the HPHT sintering TiV : VN 1 : 1 sample after annealing at 800 °C. The full-scale elemental maps are available in the SI (Fig. S5).

However, second-degree polynomial approximations of the concentration dependence of average hardness values are statistically consistent across both series (Fig. 6).

According to the results of XRD phase analysis (Table S3, SI), some HPHT-synthesized samples, in addition to the quaternary (Ti,V)(C,N) solid solution, milling contamination (α-Fe) and graphite, also contain a cubic phase with a lattice parameter of $a = 0.4124$ nm, which suggests this phase may be vanadium nitride (VN).

Microhardness data for the HPHT-sintered samples that were mechanically alloyed before sintering (Fig. 5a) were

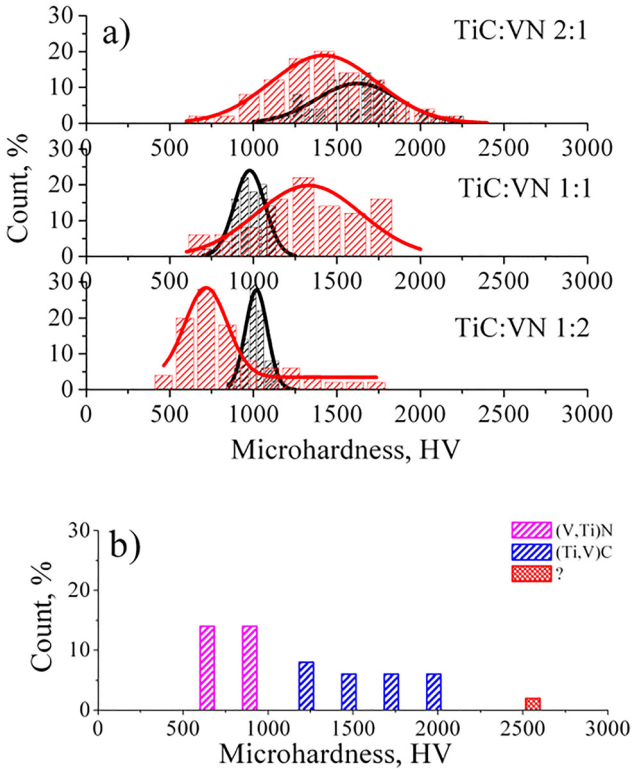

Fig. 5 Histograms of the microhardness measurement data for the samples studied and corresponding Gaussian distribution curves: HPHT-sintered samples marked as black curves; the same samples after annealing at 800 °C marked as red curves (a). Histogram of the microhardness measurement data for the HPHT-sintered TiC : VN 1 : 1 sample without prior mechanical alloying (b).

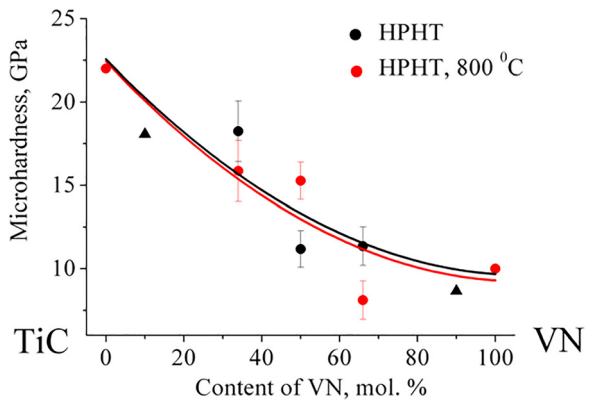

Fig. 6 Concentration dependencies of the average microhardness values of HPHT-sintered compacts containing the quaternary (Ti,V)(C,N) solid solution (circles), and data for the limiting solid solutions of (Ti,V)C and (V,Ti)N (triangles).

compared with the results for an HPHT-sintered TiC : VN 1 : 1 sample (at 2150 °C) that had not been mechanically alloyed (Fig. 5b). It is clear that statistical processing of the histogram for this untreated sample is absolutely impossible. However, the histogram can be divided into three distinct regions of different span: a lavender region spanning 590–930 HV, a blue region covering 1210–2010 HV, and a single red value at 2590 HV (29.3 GPa). Obviously, the first region corresponds to the hardness of the (V,Ti)N-based solid solution, and the second region to the (Ti,V)C-based solid solution, with average hardnesses of 8.7 and 18.1 GPa, respectively (Table S3, SI). The nature of the phase responsible for the high hardness value (~29 GPa) remains unknown. According to the XRD analysis, only solid solutions of (V,Ti)N and (Ti,V)C containing a small amount of the dissolved component were detected in this sample (see Table S2, SI). Nevertheless, individual inclusions with a composition close to $Ti_{0.25}V_{0.75}C$ may also be present; according to the theoretical calculations,[24] this phase is expected to exhibit a hardness of about 30 GPa.

A comparison of the real structure parameters and microhardness values of the samples obtained from HPHT sintering of the initial equimolar TiC : VN 1 : 1 mixture and those subjected to mechanical alloying shows that these parameters match well for titanium-rich (Ti,V)C and (Ti,V)(C,N) solid solutions (see Table S3, SI). However, certain discrepancies are observed for vanadium-rich (Ti,V)(C,N) and (V,Ti)N solid solutions.

Discussion

The results obtained in this study show that the hardness of the synthesized multicomponent (Ti,V)(C,N) composites lies in the range between that of VN nitride (≈ 12 GPa) and TiC carbide (30 GPa), amounting to 8–18 GPa (Fig. 6, Table S3 in SI). This hardness does not reach the values typical of well-known HEAs (25–50 GPa), which are mainly intended for coatings with potential applications in high-temperature structural components and cutting tools.

At present, multicomponent carbides, nitrides, and carbonitrides involving titanium and vanadium as constituents of high-entropy alloys (HEAs) have been synthesized by various methods. Notable examples include: (TiVZrHfNbTa)C carbide coatings obtained by sputtering a multicomponent alloy in the plasma of a compressed vacuum–arc discharge (hardness 43–48 GPa);[25] (TiVAlCrSiZr)N nitride coatings deposited using the co-filter cathodic vacuum arc (FCVA) technique (50.16 GPa);[26] (TiVCrZrHf)N nitride produced by rf reactive magnetron sputtering (48 GPa);[27] (TiVNbTa)(CN) carbonitride ceramics fabricated by spark plasma sintering (29.3 GPa);[28] (TiVCrAlNb)(CN) carbonitride coatings prepared by high-power impulse magnetron sputtering (32.6 GPa);[29] and (TiVNbTaMo)(CN) carbonitride powders synthesized by carbothermal reduction–nitridation followed by hot pressing at 1600–1900 °C (24.0 GPa).[30]

However, if the potential application area of the synthesized (Ti,V)(C,N) material is in medicine, its physicochemical properties are subject to specific requirements. In the case of artificial implants, key characteristics include a low elastic modulus, excellent corrosion resistance, and enhanced biocompatibility. At present, such properties are exhibited by implants based on medical-grade titanium alloy Ti–6Al–4V reinforced with TiC carbide,[7,8,31] and by biocompatible (Ti,V)N coatings.[32]

Theoretically calculated C_{12} elastic constants, which reflect the Poisson effect in cubic structures, are as follows: ≈120 GPa for TiC and ≈130 GPa for VN,[33,34] as well as ≈120 GPa for $Ti_{0.5}V_{0.5}C$ and ≈180 GPa for $Ti_{0.5}V_{0.5}N$.[34] These C_{12} values are close to the elastic modulus of Ti–6Al–4V alloys, which ranges between 110 GPa and 120 GPa.[35] Based on the reported data,[34] it can therefore be expected with a high degree of probability that the composites synthesized in this work will also exhibit similar elastic modulus values.

Previously, vanadium-rich $V_{1-x}Ti_x(C,N)$ ($0 \le x \le 0.4$) carbonitrides were synthesized *via* chemical reactions,[16] which were described in detail. Of scientific interest as well is the mechanism of solid-state formation of $V_{1-x}Ti_x(C,N)$ ($0 \le x \le 0.1$) composites.

So, in our opinion, the impact of MA, HPHT sintering, and annealing on TiC and VN, as well as on the solid solutions they form, can be explained by the thermodynamic characteristics of these phases. Specifically, increasing values of cohesive energy (6.72 eV per atom and 7.38 eV per atom for VN[36] and TiC,[37] respectively) and melting temperature (2050 and 3260 °C)[38] in the series VN → TiC explain why VN is more prone to undergo the described synthesis methods.

Thus, vanadium-rich (V,Ti)N and (Ti,V)(C,N) solid solutions form more easily and therefore have a more uniform composition of crystallites. This is particularly evident in the narrow distribution seen in the microhardness histograms of these samples (Fig. 5a, black histograms). Titanium-rich (Ti,V)C and (Ti,V)(C,N) solid solutions form more slowly and exhibit some variation in their composition (as indicated by the wider spread in the red microhardness histograms in Fig. 5a).

As shown earlier,[20,21] due to impact loading, the mechanochemical synthesis of TiC with VN leads to the formation of numerous point defects (mostly vacancies) in these phases, resulting in the accumulation of titanium and vanadium clusters in the milling reaction zone. During HPHT sintering, these clusters may not be fully incorporated into the formation of solid solutions in the quaternary (Ti,V)(C,N) solid solutions. The process of incorporating these residual clusters continues at annealing (800 °C), leading to compositional variations across different regions of the TiC : VN 1 : 1 and TiC : VN 1 : 2 samples, as detected by EDS, as well as to a broadening of the microhardness histograms (Fig. 5a).

While the present work was primarily focused on the synthesis and characterization of these composites, further investigations into their functional properties – including oxidation resistance, fracture toughness, and biocompatibility – are required. Such studies will provide the basis for evaluating their potential as modifying additives or protective coatings for biomedical titanium alloys, thereby opening new directions for their practical application.

Conclusions

HPHT sintering (7.7 GPa, 2150 °C) was conducted in a toroid-type high-pressure apparatus using three TiC–VN mixtures with molar ratios of 2 : 1, 1 : 1, and 1 : 2. These mixtures had previously undergone 9 hours of mechanochemical treatment in a high-energy planetary mill. The resulting compact samples were analyzed using XRD, SEM, and EDS techniques, leading to the following conclusions:

The sintered samples exhibited a homogeneous microstructure and consisted of nanocrystalline quaternary (Ti,V)(C,N) solid solutions. Their composition accurately matches the original TiC–VN mixture ratios, and their lattice parameters conformed well to Vegard's law. These solid solutions remained stable after 2 hours of annealing at 800 °C.

Microhardness measurements of the HPHT sintered samples followed a symmetric Gaussian distribution. Annealing at 800 °C caused a shift toward lower hardness values and broader distributions, especially for vanadium-rich compositions. The average hardness values of (Ti,V)(C,N) solid solutions decreased monotonically from 22 GPa (TiC) to 9 GPa (VN),[39] depending on composition.

HPHT sintering of an unprocessed equimolar TiC–VN mixture resulted in a sample containing two limited solid solutions, namely, (Ti,V)C and (V,Ti)N, with microhardness values of 18 GPa and 9 GPa, respectively.

Combining mechanical alloying of the initial powder charge with subsequent HPHT sintering results in the complete mutual solubility of TiC and VN phases. This leads to the formation of a single-phase composite material consisting of a quaternary (Ti,V)(C,N) solid solution whose composition corresponds to the intended blend.

Author contributions

N. M. Belyavina: contributed to conceptualization, methodology, investigation, formal analysis and visualization of the data; V. V. Kuryliuk: contributed to project administration, investigation, and data curation; A. M. Kuryliuk: contributed to investigation and validation of the experimental results; D. A. Stratiichuk: contributed to methodology, investigation, and data curation; S. P. Starik: contributed to the investigation, methodology, and validation of the experimental results, O. I. Nakonechna: contributed to conceptualization, and formal analysis. All authors equally contributed to writing the original manuscript as well as later revisions.

Conflicts of interest

There are no conflicts to declare.

Data availability

The data supporting the findings of this study are available from the corresponding author upon reasonable request.

Supplementary information is available. See DOI: **https://doi.org/10.1039/d5ma00805k**.

Acknowledgements

This work was supported by the National Research Foundation of Ukraine (grant no. 2023.05/0007), the Ministry of Education and Science of Ukraine (grant no. 240БФ051-01, registration number 0124U001075).

References

1 L. Toth, *Transition metal carbides and nitrides*, Elsevier, 2014.
2 S. A. Rasaki, B. Zhang, K. Anbalgam, T. Thomas and M. Yang, *Prog. Solid State Chem.*, 2018, **50**, 1–15.
3 M. Mhadhbi and M. Driss, *J. Brill Eng.*, 2021, **2**, 1–11.
4 E. Benko, J. S. Stanisław, B. Królicka, A. Wyczesany and T. L. Barr, *Diamond Relat. Mater.*, 1999, **8**, 1838–1846.
5 S. Y. Chiou, S. F. Ou, Y. G. Jang and K. L. Ou, *Ceram. Int.*, 2013, **39**, 1–8.
6 K. V. Slipchenko, I. A. Petrusha, V. Z. Turkevich, D. A. Stratiichuk, V. M. Slipchenko and N. M. Bilyavina, *et al.*, *Metallofiz. Noveishie Tekhnol.*, 2019, **41**, 1599–1610 (in Ukrainian).
7 H. C. Man, S. Zhang, F. T. Cheng and T. M. Yue, *Scr. Mater.*, 2001, **44**, 2801–2807.
8 W. H. Wei, Z. N. Shao, J. Shen and X. M. Duan, *Mater. Sci. Technol.*, 2018, **34**, 191–198.
9 K. Slipchenko, V. Bushlya, D. Stratiichuk, I. Petrusha, A. Can and V. Turkevich, *et al.*, *J. Eur. Ceram. Soc.*, 2022, **42**, 4513–4527.
10 N. Belyavina, V. Turkevich, D. Stratiichuk, A. Kuryliuk and O. Nakonechna, *Rep. Natl. Acad. Sci. Ukr.*, 2024, **4**, 33–47 (in Ukrainian).
11 H. Pierson, *Handbook of Refractory Carbides and Nitrides*, Noyes Publ., Westwood, 1996.
12 Y. Peng, H. Miao and Z. Peng, *Int. J. Refract. Met. Hard Mater.*, 2013, **39**, 78–89.
13 H. Holleck, *J. Vac. Sci. Technol., A*, 1986, **4**, 2661–2669.
14 D. Demirskyi, H. Borodianska, T. S. Suzuki, Y. Sakka, K. Yoshimi and O. Vasylkiv, *Scr. Mater.*, 2019, **164**, 12–16.
15 L. Feng, W. T. Chen, W. G. Fahrenholtz and G. E. Hilmas, *J. Am. Ceram. Soc.*, 2021, **104**, 419–427.
16 C. P. West, I. Harrison, E. J. Cussen and D. H. Gregory, *J. Eur. Ceram. Soc.*, 2009, **29**, 2355–2361.
17 Q. Yuan, Y. Zheng and H. Yu, *Int. J. Refract. Met. Hard Mater.*, 2009, **27**, 121–125.
18 N. Belyavina, V. Turkevich, A. Kuryliuk, D. Stratiichuk, O. Nakonechna and T. Avramenko, *et al.*, *Rep. Natl. Acad. Sci. Ukr.*, 2022, **12**, 54–63 (in Ukrainian).
19 N. Belyavina, O. Nakonechna, A. Kuryliuk, P. Kogutyuk, D. Stratiichuk and V. Turkevich, *Mater. Proc.*, 2023, **14**, 16.
20 N. M. Belyavina, A. M. Kuryliuk, V. V. Dibrov and M. P. Semenko, *Rep. Natl. Acad. Sci. Ukr.*, 2025, **1**, 3–12 (in Ukrainian).
21 N. M. Bilyavina, V. V. Kuryliuk, V. V. Dibrov and A. M. Kuryliuk, *Metallofiz. Noveishie Tekhnol.*, 2025, **47**, 1–10.
22 M. Dashevskyi, O. Boshko, O. Nakonechna and N. Belyavina, *Metallofiz. Noveishie Tekhnol.*, 2017, **39**, 541–552.
23 N. M. Belyavina, A. M. Kuryliuk, V. V. Zavodyannyi and M. P. Semenko, *J. Nano – Electron. Phys.*, 2025, **17**, 01001.
24 S. Sun, Y. Liu, H. Fu, X. Guo, S. Ma, J. Lin and R. Wang, *Adv. Eng. Mater.*, 2018, **20**, 1800295.
25 V. F. Gorban, A. A. Andreyev, G. N. Kartmazov, A. M. Chikryzhov, M. V. Karpets, A. V. Dolomanov, A. A. Ostroverkh and E. V. Kantsyr, *Sverkhtverd. Mater.*, 2017, **39**, 166–171.
26 Y. Zhao, X. Gao, X. Shi, B. Li, M. Li, W. Xie, E. Ren, Y. Chen, C. Zhang, Z. Min and B. Liao, *J. Alloys Compd.*, 2025, **1018**, 179169.
27 S.-C. Liang, Z.-C. Chang, D.-C. Tsai, Y.-C. Lin, H.-S. Sung, M.-J. Deng and F.-S. Shieu, *Appl. Surf. Sci.*, 2011, **257**, 7709–7713.
28 X. Q. Han, N. Lin, A. Q. Li, J. Q. Li, Z. G. Wu, Z. Y. Wang, Y. H. He, X. Y. Kang and C. Ma, *Ceram. Int.*, 2021, **47**, 35105–35110.
29 X. Lu, L. Yang, Y. Lu, X. Zhang, Z. Yan, J. Hao and W. Liu, *Ceram. Int.*, 2025, **51**, 13420–13429.
30 C. Jing, S.-J. Zhou, W. Zhang, Z.-Y. Ding, Z.-G. Liu, Y.-J. Wang and J.-H. Ouyang, *J. Alloys Compd.*, 2022, **927**, 167095.
31 M. Long and H. J. Rack, *Biomaterials*, 1998, **19**, 1621.
32 J. Bautista-Ruiz, A. Elhadad and W. Aperador, *Mater. Chem. Phys.*, 2024, **326**, 129856.
33 G. Sai Gautam and K. C. Hari Kumar, *J. Alloys Compd.*, 2014, **587**, 380–386.
34 S. Sun, Y. Liu, H. Fu, X. Guo, S. Ma, J. Lin, G. Guo, Y. Lei and R. Wang, *Adv. Eng. Mater.*, 2018, **20**, 1800295.
35 K. Lovera, V. Vanaclocha, C. M. Atienza, A. Vanaclocha, P. Jordá-Gómez, N. Saiz-Sapena and L. Vanaclocha, *Materials*, 2025, **18**, 700.
36 T. Fu, X. Peng, C. Huang, H. Xiang, S. Weng, Z. Wang and N. Hu, *Sci. Rep.*, 2017, **7**(1), 4768.
37 A. Vojvodic, C. Ruberto and B. I. Lundqvist, *Surf. Sci.*, 2006, **600**, 3619–3623.
38 G. V. Samsonov and I. M. Vinnitskii, *Refractory Compounds: Handbook (in Russian)*, Metallurgy, Moscow, 2nd edn, 1976.
39 S. Wang, X. Yu, J. Zhang, L. Wang, K. Leinenweber, D. He and Y. Zhao, *Cryst. Growth Des.*, 2016, **16**(1), 351–358.